# The Maximal Singularity-Free Workspace of the Gough–Stewart Platform for a Given Orientation

**Qimi Jiang**
e-mail: qimi_j@yahoo.com

**Clément M. Gosselin**
e-mail: gosselin@gmc.ulaval.ca

Department of Mechanical Engineering,
Laval University,
Quebec, QC, G1V 0A6, Canada

*The maximal singularity-free workspace of parallel mechanisms is a desirable criterion in robot design. However, for a 6DOF parallel mechanism, it is very difficult to find an analytic method to determine the maximal singularity-free workspace around a prescribed point for a given orientation. Hence, a numerical algorithm is presented in this paper to compute the maximal singularity-free workspace as well as the corresponding leg length ranges of the Gough–Stewart platform. This algorithm is based on the relationship between the maximal singularity-free workspace and the singularity surface. Case studies with different orientations are performed to demonstrate the presented algorithm. The obtained results can be applied to the geometric design or parameter (leg length) setup of this type of parallel robots.* [DOI: 10.1115/1.2976452]

*Keywords: Gough–Stewart platform, workspace sphere, singularity, maximal singularity-free workspace*

## 1 Introduction

Parallel mechanisms possess significant advantages over serial mechanisms in terms of dynamic properties, load-carrying capacity, high accuracy, as well as stiffness. However, the closed-loop nature of their architectures limits the motion of the platform and creates complex kinematic singularities inside the workspace. Hence, the maximization of the singularity-free workspace of parallel mechanisms is highly desired in the context of robot design.

Several researchers addressed the determination of the workspace based on given leg length ranges [1–5]. When the workspace is determined, the next task is to verify whether any singularity exists inside the workspace. For this purpose, the singularity equation becomes a necessary tool. Hence, several researchers have derived the singularity equations for certain types of parallel mechanisms [6–12].

However, singularity equations are difficult to obtain for mechanisms with more than three degrees of freedom (DOFs) because the determinant of the Jacobian matrix becomes very complex. For 6DOF Gough–Stewart platforms, previous studies focused on a few special cases of singularities [13–16]. Later Mayer St-Onge and Gosselin [17] and Li et al. [18] derived the singularity equations for general Gough–Stewart platforms, though the obtained singularity equations were very complex.

In order to avoid having the singularities inside the workspace, different algorithms were presented for the trajectory planning [19–23]. For instance, Merlet and Daney [23] presented a method to determine whether there is a singularity in a given region defined in the workspace. The answer is definite and can be used to identify the singularity-free zones inside the workspace. Besides this, a method was proposed in Ref. [24] to determine a singularity-free zone in the workspace of planar 3-PRR parallel mechanisms. A procedure was presented in Ref. [25] to determine a maximal singularity-free sphere around a prescribed point $P_0$ for a given orientation. This method was also extended to the six-dimensional workspace.

However, it is clear that such a maximal singularity-free sphere does not represent the real maximal singularity-free workspace. The reason is that any practical workspace cannot be a sphere for Gough–Stewart platforms. The difference between the two is shown in Fig. 1. Hence, a more interesting problem may be how to determine the maximal singularity-free workspace around a prescribed point $P_0$ for a given orientation as well as the corresponding leg length ranges. If this problem can be solved, the information obtained will be more useful in a practical context.

Unfortunately, such a maximal singularity-free workspace is very complex, especially when the given orientation is different from the reference orientation with $\phi=\theta=\psi=0$ deg (see Fig. 2). It may be affected by several factors such as the prescribed point, the given orientation angles, as well as the geometric parameters. Hence, it is very difficult to find an analytic method to determine the maximal singularity-free workspace. Instead, a numerical algorithm is presented in this work to compute the maximal singularity-free workspace as well as the corresponding leg length ranges of the Gough–Stewart platform.

## 2 Workspace Sphere

Although the algorithm presented in this work does not lose generality and can be applied to any type of Gough–Stewart platforms, the minimal simplified symmetric manipulator (MSSM) is chosen for demonstration. The reason is that the MSSM architecture has been widely used in practice because of its stability. As shown in Fig. 3, the MSSM consists of a mobile platform $P_1(P_6)P_2(P_3)P_4(P_5)$ and a base $B_1(B_2)B_3(B_4)B_5(B_6)$ connected via six identical UPS legs ($B_iP_i, i=1,2,\ldots,6$). Both the platform and the base are isosceles triangles [17].

Considering the symmetry, the fixed frame $Oxyz$ is attached to the base by selecting $B_1(B_2)$ as the origin $O$ and making the $y$ axis coincide with the line of symmetry. Besides this, the $Oxy$ plane coincides with the base triangle. Hence, the positions of $B_i(i=1,2,\ldots,6)$ in the fixed frame are, respectively, $\mathbf{b}_1=\mathbf{b}_2=[0,0,0]^T$, $\mathbf{b}_3=\mathbf{b}_4=[t_1,t_2,0]^T$, and $\mathbf{b}_5=\mathbf{b}_6=[-t_1,t_2,0]^T$. Only two geometric parameters are used to describe the base. Similarly, the mobile frame $O'x'y'z'$ is attached to the platform by selecting the midpoint of $P_1P_2$ as the origin $O'$ and $P_1P_2$ as the $x'$ axis. Besides this, the $O'x'y'$ plane coincides with the platform triangle. The positions of $P_i(i=1,2,\ldots,6)$ in the mobile frame are, respectively, $\mathbf{p}'_1=\mathbf{p}'_6=[-t_3,0,0]^T$, $\mathbf{p}'_2=\mathbf{p}'_3=[t_3,0,0]^T$, and $\mathbf{p}'_4=\mathbf{p}'_5=[0,t_4,0]^T$.

Contributed by the Mechanisms and Robotics Committee of ASME for publication in the JOURNAL OF MECHANICAL DESIGN. Manuscript received September 13, 2007; final manuscript received May 27, 2008; published online September 23, 2008. Review conducted by Qizheng Liao. Paper presented at the ASME 2007 Design Engineering Technical Conferences and Computers and Information in Engineering Conference (DETC2007), Las Vegas, NV, September 4–7, 2007.

  

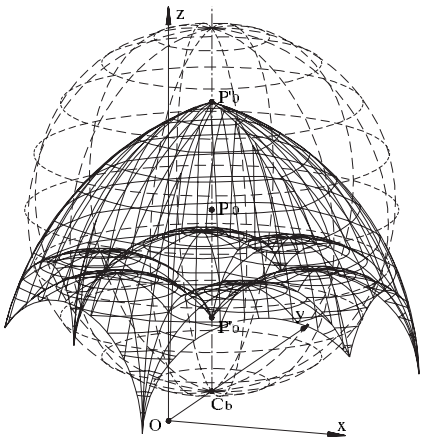


**Fig. 1 The maximal singularity-free workspace (solid) and the maximal singularity-free sphere (dashed) around $P_0(0,2\sqrt[4]{3}/3,1.25)$ at the reference orientation with $\phi=\theta=\psi=0$ deg**

Also, only two geometric parameters are used to describe the platform. Hence, the total number of geometric parameters is only 4.

Let $\mathbf{Q}$ denote the rotation matrix representing the orientation of the platform (mobile frame $O'x'y'z'$) with respect to the fixed frame $Oxyz$

$$\mathbf{Q}=\begin{bmatrix} c\theta c\psi & s\phi s\theta c\psi - c\phi s\psi & c\phi s\theta c\psi + s\phi s\psi \\ c\theta s\psi & s\phi s\theta s\psi + c\phi c\psi & c\phi s\theta s\psi - s\phi c\psi \\ -s\theta & s\phi c\theta & c\phi c\theta \end{bmatrix} \tag{1}$$

where $c\phi=\cos\phi$, $s\phi=\sin\phi$, etc. Furthermore $\phi$, $\theta$, and $\psi$ are roll-pitch-yaw angles.

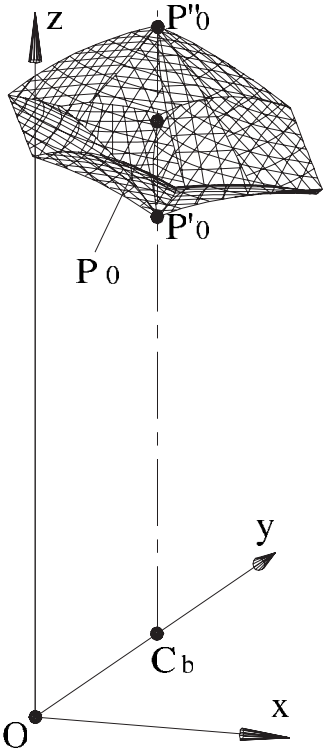


**Fig. 2 The maximal singularity-free workspace around $P_0(0,2\sqrt[4]{3}/3,1.25)$ for a given orientation with $\phi=30$ deg, $\theta=45$ deg, and $\psi=0$ deg**

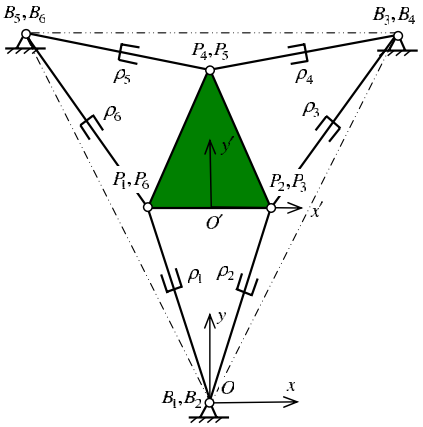


**Fig. 3 The MSSM architecture (top view)**

Let vector $\mathbf{p}_r=[x_r,y_r,z_r]^T$ denote the position of the origin $O'$ of the mobile frame in the fixed frame. The position vector of the considered point $P$ of the platform in the fixed and mobile frames is, respectively, $\mathbf{p}=[x,y,z]^T$ and $\mathbf{p}'=[x_p,y_p,z_p]^T$. One then has

$$\mathbf{p}=\mathbf{p}_r+\mathbf{Q}\mathbf{p}' \tag{2}$$

or

$$\mathbf{p}_r=\mathbf{p}-\mathbf{Q}\mathbf{p}' \tag{3}$$

Hence, the positions of $P_i(i=1,2,\ldots,6)$ in the fixed frame can be expressed as

$$\mathbf{p}_i=\mathbf{p}_r+\mathbf{Q}p_i'=\mathbf{p}+\mathbf{Q}(\mathbf{p}_i'-\mathbf{p}') \tag{4}$$

The length $\rho_i$ of leg $i$ is the distance between points $B_i$ and $P_i$. From this, one obtains

$$\rho_i^2=(\mathbf{p}_i-\mathbf{b}_i)^T(\mathbf{p}_i-\mathbf{b}_i) \tag{5}$$

Equation (5) can be expanded as follows:

$$\rho_i^2=(x+l_i)^2+(y+m_i)^2+(z+n_i)^2 \quad (i=1,2,\ldots,6) \tag{6}$$

where

$$\begin{aligned} l_i &= q_{11}(x'_{pi}-x_p)+q_{12}(y'_{pi}-y_p)+q_{13}(z'_{pi}-z_p)-x_{bi} \\ m_i &= q_{21}(x'_{pi}-x_p)+q_{22}(y'_{pi}-y_p)+q_{23}(z'_{pi}-z_p)-y_{bi} \\ n_i &= q_{31}(x'_{pi}-x_p)+q_{32}(y'_{pi}-y_p)+q_{33}(z'_{pi}-z_p)-z_{bi} \end{aligned} \tag{7}$$

and $q_{ij}(i,j=1,2,3)$ are the entries of the rotation matrix $Q$.

For a given orientation $(\phi,\theta,\psi)$, Eq. (6) represents six spheres (for $i=1,2,\ldots,6$) in the 3D Cartesian space $xyz$. These spheres can be referred to as *workspace spheres* because they can be used to determine the workspace [1]. For given leg length ranges $[\rho_i^{\min},\rho_i^{\max}]$, $(i=1,2,\ldots,6)$, when the leg lengths, respectively, take the maximal and the minimal leg lengths, there will be 12 workspace spheres. These 12 spheres will define the boundary of the workspace. In other words, the workspace lies inside six spheres whose radii are the maximal leg lengths $\rho_i^{\max}(i=1,2,\ldots,6)$, and outside another six spheres whose radii are the minimal leg lengths $\rho_i^{\min}(i=1,2,\ldots,6)$.

From Eq. (6), the centers $C_i(x_{ci},y_{ci},z_{ci})$, $(i=1,2,\ldots,6)$ of the workspace spheres can be given as follows:

$$\begin{aligned} x_{ci} &= -l_i \\ y_{ci} &= -m_i \quad (i=1,2,\ldots,6) \\ z_{ci} &= -n_i \end{aligned} \tag{8}$$

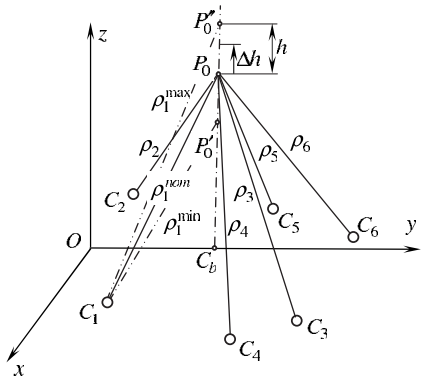


**Fig. 4 Workspace around a prescribed point $P_0$**

## 3 Singularity Equation

Differentiating Eq. (5) with respect to time, one obtains

$$\rho_i\dot{\rho}_i = (\mathbf{p}_i - \mathbf{b}_i)^T\dot{\mathbf{p}} + [\mathbf{Q}(\mathbf{p}_i' - \mathbf{p}') \times (\mathbf{p}_i - \mathbf{b}_i)]^T\boldsymbol{\omega} \tag{9}$$

where $\boldsymbol{\omega}$ is the angular velocity of the platform. For all six legs, Eq. (9) can be rewritten as follows:

$$\mathbf{A}\mathbf{v} = \mathbf{D}\dot{\boldsymbol{\rho}} \tag{10}$$

where $\dot{\boldsymbol{\rho}}=[\dot{\rho}_1, \dot{\rho}_2, \ldots, \dot{\rho}_6]^T$ denotes the actuator velocities and $\mathbf{v}=[\dot{\mathbf{p}}^T, \boldsymbol{\omega}^T]^T$ denotes the Cartesian velocity vector of the platform. $\mathbf{A}$ and $\mathbf{D}$ are two Jacobian matrices and $\mathbf{D}=\text{diag}(\rho_1, \rho_2, \ldots, \rho_6)$.

The singularity condition is $\det(\mathbf{A})=0$. Similar to Refs. [17,18], the determinant of matrix $\mathbf{A}$ can be expanded using linear decomposition. Hence, the singularity equation obtained can be given as follows:

$$f_1x^2z + f_2x^2 + f_3xyz + f_4xy + f_5xz^2 + f_6xz + f_7x + f_8y^2z + f_9y^2 + f_{10}yz^2 + f_{11}yz + f_{12}y + f_{13}z^3 + f_{14}z^2 + f_{15}z + f_{16} = 0 \tag{11}$$

where $f_i=f_i(\phi, \theta, \psi)$, $(i=1,2,\ldots,16)$.

By substituting Eq. (8) into Eq. (11), it is readily observed that the six centers lie exactly on the singularity locus.

## 4 Maximal Singularity-Free Workspace

**4.1 Workspace Around $\mathbf{P_0}$.** By strict definition, the workspace around a prescribed point $P_0(x_0, y_0, z_0)$ should be a region:

- that can be reached by the end-effector for given leg length ranges and
- where $P_0$ lies exactly at the centroid

However, such a workspace is very difficult to define in practice because the shape of any practical workspace is very complex. Instead of the strict definition, this work defines it as shown in Fig. 4. Considering that $C_i(i=1,2,\ldots,6)$ are the six centers of the workspace spheres, the workspace around a prescribed point $P_0$ is a region:

- that can be reached by the end-effector for given leg length ranges and
- where $P_0$ lies at the midpoint of the segment $P_0'P_0''$, which is perpendicular to the base and is inside the workspace. $P_0'$ and $P_0''$, respectively, lie on the downside and upside boundaries of the workspace.

The length of $\overline{P_0'P_0''}$ is referred to as the height of the workspace along this perpendicular line or in short the height of the workspace. Obviously, this height is not necessarily the whole height of the workspace (see Fig. 5(*a*)). But this quantity is very important because it determines the size of the workspace. For convenience, instead of using this quantity directly, the half height denoted by $h$ will be more useful. Obviously, $h$ is the length of $P_0P_0''$ $(=P_0'P_0)$.

As shown in Fig. 4, the distance between the center $C_i(i=1,2,\ldots,6)$ and the prescribed point $P_0$ is referred to as the nominal leg length $\rho_i^{nom}$. When the half height $h$ is given, the maximal and minimal leg lengths can be determined. Figure 4 shows that the maximal leg length $\rho_i^{max}$ should be equal to $\overline{C_iP_0''}$ and the minimal leg length $\rho_i^{min}$ should be equal to $\overline{C_iP_0'}$. However, this is not always the case. Under some orientations, the center $C_i$ may be higher than the prescribed point $P_0$. In this case, $\overline{C_iP_0'} > \overline{C_iP_0''}$. Hence, the maximal leg length $\rho_i^{max}=\max(\overline{C_iP_0'}, \overline{C_iP_0''})$. For the minimal leg length $\rho_i^{min}$, if the center $C_i$ is higher than $P_0'$ and lower than $P_0''$, $\rho_i^{min}$ will be the perpendicular distance from $C_i$ to the line $P_0'P_0''$. Otherwise, $\rho_i^{min}=\min(\overline{C_iP_0'}, \overline{C_iP_0''})$.

**4.2 Maximal Singularity-Free Workspace Around $\mathbf{P_0}$.** The maximal singularity-free workspace around the prescribed point $P_0(x_0, y_0, z_0)$ is the maximal workspace around this point in which no singular configuration exists. In this case, the half height $h$ reaches its limit value $h_{lim}$ so that the boundary of the workspace just touches the singularity surface at some point(s).

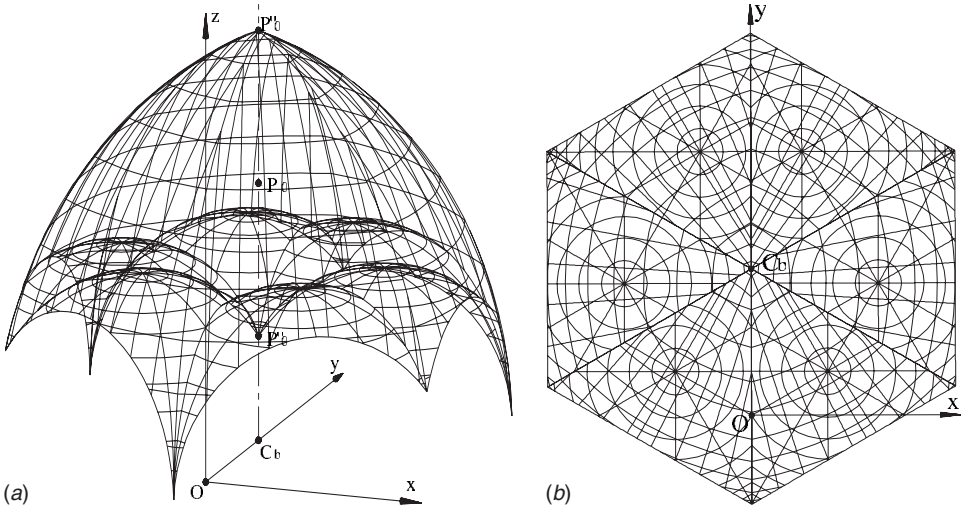


**Fig. 5 The maximal singularity-free workspace around $P_0(0, 2\sqrt[4]{3}/3, \frac{5}{4})$ for a given orientation with $\phi=\theta=\psi=0$ deg**

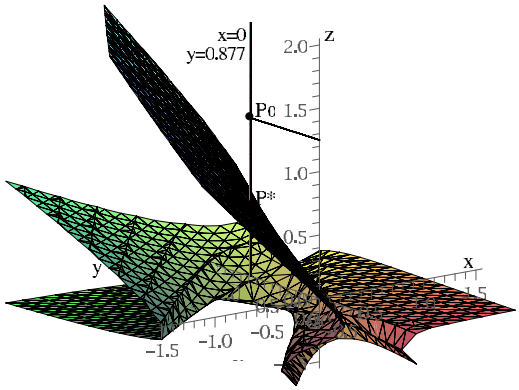


**Fig. 6 The singularity surface for a given orientation with $\phi$ =30 deg, $\theta$=45 deg, and $\psi$=0 deg**

However, there are two cases that make the maximal singularity-free workspace vanish. One case is that the prescribed point $P_0$ lies exactly on the singularity surface. Another case is that the prescribed point $P_0$ lies in the $Oxy$ plane, because in practice $P_0$ should be above the $Oxy$ plane.

## 5 Numerical Algorithm

**5.1 Basic Principle.** The maximal singularity-free workspace can be determined by the limit value $h_{\lim}$ of the half height $h$. However, it is very difficult to determine $h_{\lim}$ analytically because it may be affected by several factors, such as the prescribed point, the given orientation angles, as well as the geometric parameters. Hence, a numerical algorithm is presented to solve this problem. The basic principle of the algorithm can be stated as follows. Increase the half height $h$ from 0 until the boundary of the workspace touches the singularity surface. Referring to Fig. 4, the general procedure can be described as follows. First, set the half height $h$ to 0. Then, increase $h$ by one step $\Delta h$ and verify whether any singularity exists inside the obtained workspace. If no singularity exists, continue to increase $h$ with the same step size $\Delta h$. Otherwise, the used step size is too large for this step. Then, restore $h$ to its previous value and reduce the step size $\Delta h$ by one half. Then, increase $h$ by the reduced step size $\Delta h$. Repeat this procedure until the half height $h$ converges to its limit value $h_{\lim}$. At this moment, the step size $\Delta h$ becomes very small and the singularity-free workspace reaches the maximum. The detailed procedure is given in the Appendix.

In order to make the above procedure more efficient, the initial value of the step size $\Delta h$ is not necessarily very small. Actually, it can be chosen as follows (see Fig. 6). First, compute the intersection $P^*(x_0, y_0, z^*)$ between the line perpendicular to the base ($x=x_0, y=y_0$) and the singularity surface. If $z_0 > z^*$ as shown in Fig. 6, then $\Delta h = z_0 - z^*$. Otherwise, $\Delta h = \min\{z_0, (z^* - z_0)\}$.

**5.2 Workspace Volume.** For every given half height $h$, there exists a workspace. To guarantee no singularity inside the obtained workspace, it is necessary to perform singularity verification. However, in the 3D Cartesian space $Oxyz$, both the workspace and the singularity surface are very complex. To verify the singularity in the 3D Cartesian space $Oxyz$ is not convenient. Comparatively, the singularity verification in a 2D workspace section for a given value of $z$ is easy. If every workspace section is singularity-free, the entire workspace should be singularity-free.

However, there are infinitely many workspace sections, it is impossible to verify every one. One solution to this problem is to verify only a few workspace sections, which are used to evaluate the workspace volume. The density of these workspace sections depends on the convergence precision. In other words, when the workspace volume converges to a given precision, the two neighboring workspace sections can be regarded as sufficiently close. For a given half height $h$, the workspace volume $V$ can be given as

$$V \approx \sum_{i=0}^{n-1} \frac{(A_i + A_{i+1})\Delta z}{2} \tag{12}$$

where $A_i (i=0,1,\ldots,n)$ is the area of the $i$th workspace section.

However, the number $n$ is hard to determine because the $z$ coordinates of the highest and lowest points of the workspace are unknown. Considering that point $P_0(x_0, y_0, z_0)$ always lies inside the workspace, a valid workspace section should exist in the plane with $z=z_0$. Hence, the workspace can be divided into two parts: the upside part with $z \geq z_0$ and the downside part with $z \leq z_0$. Take the upside part as an example, its volume $V_1$ can be given as

$$V_1 \approx \sum_{i=0}^{n_1-1} \frac{(A_i + A_{i+1})\Delta z}{2} \tag{13}$$

where $A_0$ is the area of the workspace section with $z=z_0$. The number $n_1$ can be determined as follows. For a given step size $\Delta z$, $n_1$ is the maximal number of the steps for $z$ to increase from $z_0$ until a value $(z_0 + n_1 \Delta z)$ at which the corresponding workspace section vanishes, i.e., $A_{n_1} = 0$.

The volume $V_2$ of the downside part can be computed in a similar way. When $V_1$ and $V_2$ are available, their sum is the volume $V$ of the entire workspace.

Hence, the computation of the workspace volume is twofold. When the half height $h$ has not reached its limit value $h_{\lim}$, the objective is to perform singularity verification. When $h$ reaches its limit value $h_{\lim}$, the volume of the maximal singularity-free workspace is obtained. Obviously, if $h$ exceeds its limit value $h_{\lim}$, the singularity curve will be found in some workspace section. The computation of the workspace volume will not continue. In this case, $h$ is restored to its previous value and the step size $\Delta h$ is reduced. Then, the new step size $\Delta h$ is used to increase the half height $h$.

**5.3 Workspace Section.** To compute the workspace and to verify whether any singularity exists inside the workspace, it is necessary to define the workspace section. If the workspace section exists in the plane with a given $z$, the sections of the maximal workspace sphere with radius $\rho_i^{\max}$ and the minimal workspace sphere with radius $\rho_i^{\min}$ are two circles, respectively, with radii

$$r_{zi\,\max} = \sqrt{\rho_{i\,\max}^2 - (z - z_{ci})^2}$$

$$r_{zi\,\min} = \sqrt{\rho_{i\,\min}^2 - (z - z_{ci})^2} \tag{14}$$

There is a possible total of 12 circles in a section. Hence, the workspace section should be a region in which any point $(x, y)$ has to satisfy the following condition:

$$r_{zi\,\min} \leq \sqrt{(x - x_{ci})^2 + (y - y_{ci})^2} \leq r_{zi\,\max} \tag{15}$$

The boundary of the workspace section can be defined with the method used in Ref. [1].

**5.4 Singularity Verification.** The singularity verification can be implemented in the workspace section. The rationale is as follows: If no singularity exists inside every workspace section, as long as two neighboring workspace sections are sufficiently close, it can be guaranteed under a given precision that no singularity exists inside the workspace.

In the workspace section plane with a given $z$, the singularity locus can be given by a quadratic curve as

$$ax^2 + bxy + cy^2 + dx + ey + g = 0 \tag{16}$$

where

$$a = f_1 z + f_2$$

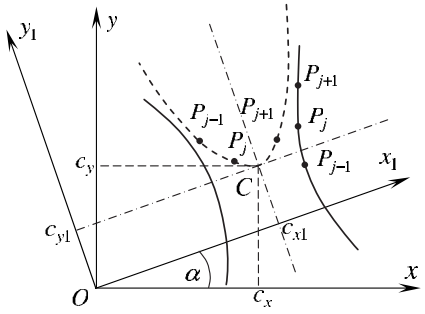


**Fig. 7 Coordinate transformation**

$$b = f_3 z + f_4$$

$$c = f_8 z + f_9$$

$$d = f_5 z^2 + f_6 z + f_7$$

$$e = f_{10} z^2 + f_{11} z + f_{12}$$

$$g = f_{13} z^3 + f_{14} z^2 + f_{15} z + f_{16} \tag{17}$$

The singularity verification can be performed as follows. First, separate the singularity curve into several arcs by computing the intersections with the 12 section circles determined in Sec. 53. Then, verify whether any obtained arc lies inside the workspace section.

The singularity curve given by Eq. (16) may be an ellipse ($b^2-4ac<0$), a parabola ($b^2-4ac=0$), or a hyperbola ($b^2-4ac>0$). For a general quadratic curve, it is inconvenient to compute the intersections with the 12 section circles. Even if all intersections are available, it is still difficult to set them in order and use them to separate the singularity curve into reasonable arcs. In order to solve this problem, a coordinate transformation is necessary (see Fig. 7 in which the case of an ellipse is not shown). The objective is to make the $y_1$ axis of the new frame $Ox_1y_1$ parallel to one axis of the ellipse, the symmetric line of the parabola, or the symmetric line of the hyperbola, which separates the hyperbola into two independent curves. To achieve this point, the cross term in $xy$ has to vanish.

Suppose the rotation angle is $\alpha$, the coordinate relationship can be expressed as

$$x = x_1 \cos\alpha - y_1 \sin\alpha$$

$$y = x_1 \sin\alpha + y_1 \cos\alpha \tag{18}$$

By substituting Eq. (18) into Eq. (16), one obtains

$$a_1 x_1^2 + b_1 x_1 y_1 + c_1 y_1^2 + d_1 x_1 + e_1 y_1 + g = 0 \tag{19}$$

where

$$a_1 = a\cos^2\alpha + b\sin\alpha\cos\alpha + c\sin^2\alpha$$

$$b_1 = (c-a)\sin 2\alpha + b\cos 2\alpha$$

$$c_1 = a\sin^2\alpha - b\sin\alpha\cos\alpha + c\cos^2\alpha$$

$$d_1 = d\cos\alpha + e\sin\alpha$$

$$e_1 = e\cos\alpha - d\sin\alpha \tag{20}$$

To make the cross term vanish, $b_1$ should be equal to 0. From this, one obtains

$$\alpha = \frac{\arctan\left(\frac{b}{a-c}\right)}{2}, \quad \alpha \in (-\pi/2, \pi/2) \tag{21}$$

Hence, after a rotation $\alpha$ of the coordinate frame, the singularity curve can be given in the new frame as

$$a_1 x_1^2 + c_1 y_1^2 + d_1 x_1 + e_1 y_1 + g = 0 \tag{22}$$

However, the above operation does not guarantee that the objective of the coordinate transformation has been achieved completely. The following cases still need to be addressed:

- $a_1 c_1 = 0$. The singularity curve is a parabola. If $a_1 \neq 0$, $y_1 = -(a_1 x_1^2 + d_1 x_1 + g)/e_1$, which is a parabola with the symmetric line parallel to the $y_1$ axis, as shown in Fig. 7. If $c_1 \neq 0$, the symmetric line will be parallel to the $x_1$ axis. To make the symmetric line parallel to the $y_1$ axis, the rotation angle needs to be changed by $\pi/2$. If $\alpha > 0$, reduce $\alpha$ by $\pi/2$. Otherwise, increase $\alpha$ by $\pi/2$.
- $a_1 c_1 \neq 0$. In this case, Eq. (22) can be rewritten as

$$\frac{(x_1 - c_{x1})^2}{a_0} + \frac{(y_1 - c_{y1})^2}{b_0} = 1 \tag{23}$$

where

$$c_{x1} = -d_1/(2a_1)$$

$$c_{y1} = -e_1/(2c_1)$$

$$a_0 = (d_1^2/a_1 + e_1^2/c_1 - 4g)/(4a_1)$$

$$b_0 = (d_1^2/a_1 + e_1^2/c_1 - 4g)/(4c_1) \tag{24}$$

If $a_0 b_0 > 0$, the singularity curve is an ellipse. Else, the singularity curve is a hyperbola. If $a_0 > 0$ and $b_0 < 0$, the hyperbola is the same as that shown in Fig. 7 and can be decomposed into two independent curves: $x_1 = c_{x1} + \sqrt{a_0[1-(y_1-c_{y1})^2/b_0]}$ and $x_1 = c_{x1} - \sqrt{a_0[1-(y_1-c_{y1})^2/b_0]}$. If $a_0 < 0$ and $b_0 > 0$, the symmetric line separating the hyperbola into two curves is parallel to the $x_1$ axis. To make it parallel to the $y_1$ axis, the rotation angle needs to be changed by $\pi/2$. If $\alpha > 0$, reduce $\alpha$ by $\pi/2$. Otherwise, increase $\alpha$ by $\pi/2$.

Besides this, the 12 section circles also need to be transformed into the new frame using Eq. (18). Then, the intersections of the singularity curve and the 12 section circles can be computed in the new frame $Ox_1y_1$. When all intersections are available, they can be easily ordered to separate the singularity curve into reasonable arcs. For an ellipse, the ordering operation can be performed using the angle between the line $CP_j$ and the $x_1$ axis. For a parabola, the ordering operation can be performed using the $x_1$ coordinate of every intersection. For a hyperbola, the ordering operation can be performed, respectively, with its two independent curves using the $y_1$ coordinate of every intersection. After the singularity curve is separated into several arcs, it is easy to verify whether any of these arcs is inside the workspace section or not.

## 6 Case Studies

In order to demonstrate the proposed algorithm, consider a MSSM with an equilateral triangle base of unit area. Suppose that the platform is also an equilateral triangle and the size ratio between the platform and the base is $\frac{3}{5}$. Hence, the geometric parameters are as follows: $t_1 = 1/\sqrt[4]{3}$, $t_2 = \sqrt[4]{3}$, $t_3 = 3/5\sqrt[4]{3}$, and $t_4 = 3\sqrt[4]{3}/5$. Take the centroid of the platform as the considered point (end-effector) $P$. Its position in the mobile frame $O'x'y'z'$ is given as $\mathbf{p}' = [0, \sqrt[4]{3}/5, 0]^T$.

In practice, the interesting workspace of the end-effector should be located above the base. Furthermore the most interesting posi-

**Table 1 The six centers of the workspace spheres for a given orientation with $\phi=\theta=\psi=0$ deg**

| $C_i$ | 1 | 2 | 3 | 4 | 5 | 6 |
|---|---|---|---|---|---|---|
| $x_{ci}$ | $3/5\sqrt[4]{3}$ | $-3/5\sqrt[4]{3}$ | $2/5\sqrt[4]{3}$ | $1/\sqrt[4]{3}$ | $-1/\sqrt[4]{3}$ | $-2/5\sqrt[4]{3}$ |
| $y_{ci}$ | $\sqrt[4]{3}/5$ | $\sqrt[4]{3}/5$ | $6\sqrt[4]{3}/5$ | $3\sqrt[4]{3}/5$ | $3\sqrt[4]{3}/5$ | $6\sqrt[4]{3}/5$ |
| $z_{ci}$ | 0 | 0 | 0 | 0 | 0 | 0 |

tion may be on the perpendicular line through the centroid $C_b(0,2\sqrt[4]{3}/3,0)$ of the base. This line can be given as

$$x=0$$

$$y=\frac{2\sqrt[4]{3}}{3}\approx 0.877$$

$$z>0 \tag{25}$$

For an equilateral triangle base of unit area, the length of the three sides is $2/\sqrt[4]{3}\approx 1.520$. Hence, the most interesting position for $P_0(x_0,y_0,z_0)$ may be on the line given by Eq. (25) with $0.8\leq z_0\leq 2$. The following case studies with different orientations will focus on point $P_0$ at $(0,2\sqrt[4]{3}/3,1.25)$.

**6.1 Case 1: $\phi=\theta=\psi=0$ deg.** In this case, the singularity surface becomes a plane, which coincides with the $Oxy$ plane. The six centers of the workspace spheres are listed in Table 1. It can be seen that all six centers lie exactly in the $Oxy$ plane.

The determined maximal singularity-free workspace is represented in Fig. 5, which looks like an umbrella, and is symmetric about the plane perpendicular to the base through the $y$ axis. The numerical results are listed in Table 2. The initial step sizes used are $\Delta h=1.25$ and $\Delta z=0.05$. The final step sizes become $\Delta h=1.907349\times 10^{-5}$ and $\Delta z=1.160473\times 10^{-4}$. The lowest points with $z=0.002724$ are very close to the singularity surface (the $Oxy$ plane). These points correspond to three of the six tips, not the point $P_0'$ with $z_0'=0.507298$. In this case, the leg length ranges for all six legs are the same [0.917823, 2.134458] because of the symmetry. The nominal leg length is $\rho_i^{\text{nom}}=1.465452$ ($i=1,2,\ldots,6$).

As the singularity surface becomes a plane coinciding with the $Oxy$ plane, it is easy to determine the maximal singularity-free sphere around $P_0$, as shown in Fig. 1.

**6.2 Case 2: $\varphi=30$ deg, $\theta=45$ deg, and $\psi=0$ deg.** In this case, the singularity surface in the 3D Cartesian space $xyz$ is shown in Fig. 6. It can be seen that the singularity surface intersects the line given by Eq. (25) at $z=0.577$. The six centers of the workspace spheres are listed in Table 3. It can be seen that the six centers do not lie in one plane because they lie on the singularity surface, which is no longer a plane. $C_1$ and $C_6$ and $C_4$ and $C_5$, respectively, lie in two different planes, which are parallel to and lower than the base. $C_2$ and $C_3$ lie in another plane, which is parallel to and higher than the base.

The determined maximal singularity-free workspace is represented in Fig. 2, which looks like a diamond and is no longer symmetric. The numerical results are listed in Table 4. The initial step sizes used are $\Delta h=1.25-0.577=0.673$ and $\Delta z=0.05$. The final step sizes become $\Delta h=1.192093\times 10^{-6}$ and $\Delta z=5.838186\times 10^{-4}$. The leg lengths are listed in Table 5. It can be seen that in this case, the leg length ranges for all six legs are different from

**Table 2 Numerical results for a given orientation with $\phi=\theta=\psi=0$ deg**

| $V$ | $h_{\text{lim}}$ | $\Delta h$ | $\Delta z$ | $z_{\max}$ | $z_{\min}$ |
|---|---|---|---|---|---|
| 2.758013 | 0.742702 | $1.907349\times 10^{-5}$ | $1.160473\times 10^{-4}$ | 1.992702 | 0.002724 |

**Table 3 The six centers of the workspace spheres for a given orientation with $\phi=30$ deg, $\theta=45$ deg, and $\psi=0$ deg**

| $C_i$ | 1 | 2 | 3 | 4 | 5 | 6 |
|---|---|---|---|---|---|---|
| $x_{ci}$ | 0.415 | −0.229 | 0.531 | 0.574 | −0.946 | −0.344 |
| $y_{ci}$ | 0.228 | 0.228 | 1.544 | 0.860 | 0.860 | 1.544 |
| $z_{ci}$ | −0.229 | 0.415 | 0.415 | −0.186 | −0.186 | −0.229 |

**Table 4 Numerical results for a given orientation with $\phi=30$ deg, $\theta=45$ deg, and $\psi=0$ deg**

| $V$ | $h_{\text{lim}}$ | $\Delta h$ | $\Delta z$ | $z_{\max}$ | $z_{\min}$ |
|---|---|---|---|---|---|
| 0.063893 | 0.233527 | $1.192093\times 10^{-6}$ | $5.838186\times 10^{-4}$ | 1.483527 | 1.016473 |

**Table 5 Leg lengths for a given orientation with $\phi=30$ deg, $\theta=45$ deg, and $\psi=0$ deg**

| No. | 1 | 2 | 3 | 4 | 5 | 6 |
|---|---|---|---|---|---|---|
| $\rho_{\text{nom}}$ | 1.668144 | 1.082058 | 1.192633 | 1.546573 | 1.719760 | 1.658730 |
| $\rho_{\max}$ | 1.878339 | 1.270895 | 1.366271 | 1.765551 | 1.919077 | 1.869984 |
| $\rho_{\min}$ | 1.465033 | 0.914109 | 1.042650 | 1.332545 | 1.530151 | 1.454304 |

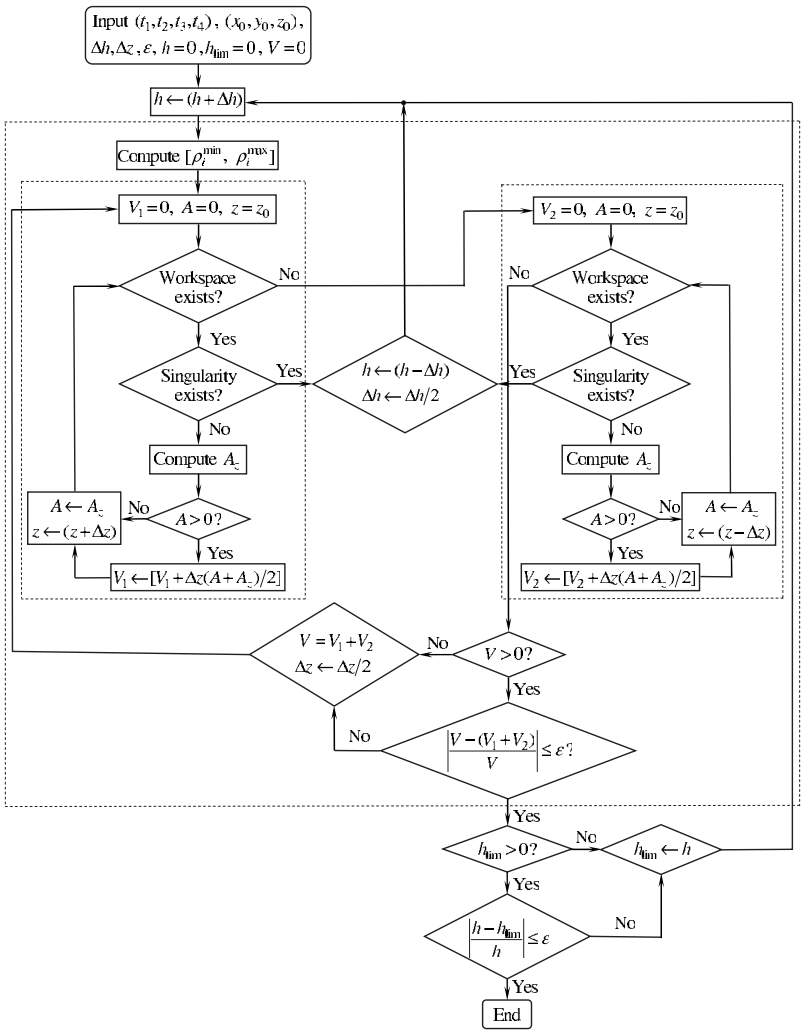


**Fig. 8 Procedure for determining the maximal singularity-free workspace**

one another because of the effect of the orientation. Comparing this with Case 1, the volume of the maximal singularity-free workspace in this case becomes very small.

**6.3 Computational Cost.** The presented algorithm was programmed using VISUAL C++ 6.0 in a Windows XP environment. The CPU of the computer is a Pentium IV with 2.4 GHz. The computational time at the given convergence precision of $\varepsilon = 10^{-4}$ is about 4 s. If the convergence precision is improved to $\varepsilon = 10^{-5}$, the computational time will be approximately 7 s for Case 2, for example. However, the results do not change in the first six digits after the decimal point. For instance, the value of $h_{\lim}$ will change from 0.2335274220 to 0.2335274965. The increment is only $7.45 \times 10^{-8}$. Hence, $\varepsilon = 10^{-4}$ is already a good convergence precision with an acceptable computational cost.

## 7 Conclusions

This work proposed a general algorithm to determine the maximal singularity-free workspace around a point of interest for the Gough–Stewart platform with a given orientation. As the shape and the size of the workspace may be affected by several factors, it is very difficult to obtain an analytic solution for this problem. Instead, an numerical algorithm is presented in this work to compute the maximal singularity-free workspace as well as the corresponding leg length ranges. Case studies with different orientations are performed to demonstrate the presented algorithm. The obtained results can be applied to the geometric design or parameter (leg length) setup of this type of parallel robots.

Although this work uses the MSSM architecture for demonstration, the presented algorithm does not lose generality and can be applied to any type of Gough–Stewart platforms.


## Acknowledgment

The authors would like to acknowledge the financial support of the Natural Sciences and Engineering Research Council of Canada (NSERC) as well as the Canada Research Chair (CRC) Program.


## Appendix: The Computational Procedure

The procedure for computing the maximal singularity-free workspace around a prescribed point at a given orientation is given in Fig. 8. The big dashed rectangular frame represents the computation of the volume $V$ of the singularity-free workspace for a given half height $h$. It contains two small dashed rectangular frames. The left one is for computing the upside part of the singularity-free workspace, $V_1$. Furthermore the right one is for computing the downside part of the singularity-free workspace, $V_2$. When $h$ converges to its limit value $h_{\lim}$, $V$ reaches the maximum. Details are given as follows.

*Step 1.* Input the geometric parameters $(t_1,t_2,t_3,t_4)$, the coordinates $(x_0,y_0,z_0)$ of the prescribed point $P_0$, the step sizes $\Delta h$ (for

determining $h_{\lim}$) and $\Delta z$ (for computing $V$), and the convergence precision $\varepsilon$. Set the initial values of $h$, $h_{\lim}$, and $V$ to 0.

*Step 2.* Increase $h$ by $\Delta h$ and compute the leg length ranges $[\rho_i^{\min}, \rho_i^{\max}]$, $(i=1,2,\ldots,6)$.

*Step 3.* Compute $V_1$.

*Step 3.1.* Set the initial values of $V_1$ and $A$ to 0. Here, $A$ denotes the area of the workspace section at $(z-\Delta z)$. Let $z$ be $z_0$, which means that the computation starts from the workspace section at $z=z_0$.

*Step 3.2.* Determine the workspace section at $z$ using the approach mentioned in Sec. 53. If the workspace section does not exist, go to Step 4.

*Step 3.3.* Perform singularity verification using the approach mentioned in Sec. 54. If a singularity exists inside the workspace section, restore the previous value of $h$ and reduce the step size $\Delta h$ by one half, then go to Step 2.

*Step 3.4.* Compute the area $A_z$ of the workspace section using the Gauss divergence theorem [1].

*Step 3.5.* If $A>0$, increase the volume $V_1$ by $\Delta z(A+A_z)/2$.

*Step 3.6.* Give the value of $A_z-A$ and increase $z$ by $\Delta z$. Then, go to Step 3.2.

*Step 4.* Compute the downside part of the singularity-free workspace, $V_2$, using the similar procedure given in the right dashed rectangular frame.

*Step 5.* If $V>0$, verify the convergence condition. If $V$ has already reached the desired precision, go to Step 7.

*Step 6.* Put the sum of $V_1$ and $V_2$ in $V$. Then, reduce the step size $\Delta z$ by one half in order to improve the precision and go to Step 3.

*Step 7.* If $h_{\lim}>0$, verify the convergence condition. If the convergence condition is satisfied, output the results and end the computation.

*Step 8.* Set the value of $h$ to $h_{\lim}$ and go to Step 2.

The above procedure shows that the workspace is determined by the half height $h$. If there is no singularity inside the workspace, continue to increase $h$ using the same step size $\Delta h$. Otherwise, restore $h$ to its previous value. Then, reduce the step size $\Delta h$ by one half and increase $h$ by the new step size. Repeat this procedure until $h$ converges to its limit value $h_{\lim}$.

To guarantee no singularity inside the workspace determined by a given $h$, the distance $\Delta z$ between two neighboring sections should also be sufficiently small. Furthermore this is controlled by the convergence condition of the workspace volume $V$. In other words, the convergence condition for $V$ serves two purposes: to make the computed $V$ achieve the desired precision and to guarantee a singularity-free workspace.

## References


[1] Gosselin, C., 1990, "Determination of the Workspace of 6-DOF Parallel Manipulators," ASME J. Mech. Des., **112**, pp. 331–336.

[2] Merlet, J.-P., 1999, "Determination of 6D Workspaces of Gough-Type Parallel Manipulator and Comparison Between Different Geometries," Int. J. Robot. Res., **18**(9), pp. 902–916.

[3] Monsarrat, B., and Gosselin, C., 2003, "Workspace Analysis and Optimal Design of a 3-leg 6-DOF Parallel Platform Mechanism," IEEE Trans. Rob. Autom., **19**(6), pp. 954–956.

[4] Huang, T., Wang, J., and Whitehouse, D., 1999, "Closed Form Solution to Workspace of Hexapod-Based Virtual Axis Machine Tools," ASME J. Mech. Des., **121**(1), pp. 26–31.

[5] Pernkopf, F., and Husty, M., 2006, "Workspace Analysis of Stewart–Gough-Type Parallel Manipulators," Proc. Inst. Mech. Eng., Part C: J. Mech. Eng. Sci., **220**(7), pp. 1019–1032.

[6] Gosselin, C., and Angeles, J., 1990, "Singularity Analysis of Closed-Loop Kinematic Chains," IEEE Trans. Rob. Autom., **6**(3), pp. 281–290.

[7] Zlatanov, D., Fenton, R. G., and Behhabid, B., 1994, "Singularity Analysis of Mechanisms and Robots Via a Velocity-Equation Model of the Instantaneous Kinematics," *Proceedings of the IEEE International Conference on Robotics and Automation*, San Diego, CA, May 8–13, pp. 986–991.

[8] Sefrioui, J., and Gosselin, C., 1995, "On the Quadratic Nature of the Singularity Curves of Planar Three-Degree-Of-Freedom Parallel Manipulators," Mech. Mach. Theory, **30**(4), pp. 533–551.

[9] Wang, J., and Gosselin, C., 2004, "Singularity Loci of a Special Class of Spherical 3D of Parallel Mechanisms With Prismatic Actuators," ASME J. Mech. Des., **126**(2), pp. 319–326.

[10] Bonev, I., Zlatanov, D., and Gosselin, C., 2003, "Singularity Analysis of 3-DOF Planar Parallel Mechanisms Via Screw Theory," ASME J. Mech. Des., **125**(3), pp. 573–581.

[11] Huang, Z., Cao, Y., Li, Y., and Chen, L., 2006, "Structure and Property of the Singularity Loci of the 3/6-Stewart–Gough Platform for General Orientations," Robotica, **24**, pp. 75–84.

[12] Collins, C. L., and McCarthy, J. M., 1998, "The Quartic Singularity Surfaces of Planar Platforms in the Clifford Algebra of the Projective Plane," Mech. Mach. Theory, **33**(7), pp. 931–944.

[13] Fichter, E. F., 1986, "A Stewart Platform-Based Manipulator: General Theory and Practical Construction," Int. J. Robot. Res., **5**(2), pp. 157–182.

[14] Merlet, J.-P., 1989, "Singular Configurations of Parallel Manipulators and Grassmann Geometry," Int. J. Robot. Res., **8**(5), pp. 45–56.

[15] Hunt, K. H., and McAree, P. R., 1998, "The Octahedral Manipulator: Geometry and Mobility," Int. J. Robot. Res., **17**(8), pp. 868–885.

[16] McAree, P. R., and Daniel, R. W., 1999, "An Explanation of Never-Special Assembly Changing Motions For 3-3 Parallel Manipulators," Int. J. Robot. Res., **18**(6), pp. 556–574.

[17] Mayer St-Onge, B., and Gosselin, C., 2000, "Singularity Analysis and Representation of the General Gough–Stewart Platform," Int. J. Robot. Res., **19**(3), pp. 271–288.

[18] Li, H., Gosselin, C., Richard, M., and Mayer-St-Onge, B., 2006, "Analytic Form of the Six-Dimensional Singularity Locus of the General Gough–Stewart Platform," ASME J. Mech. Des., **128**(1), pp. 279–287.

[19] Merlet, J.-P., 1994, "Trajectory Verification in the Workspace for Parallel Manipulator," Int. J. Robot. Res., **13**(4), pp. 326–333.

[20] Bhattacharya, S., Hatwal, H., and Ghosh, A., 1998, "Comparison of an Exact and an Approximate Method of Singularity Avoidance in Platform Type Parallel Manipulators," Mech. Mach. Theory, **33**(7), pp. 965–974.

[21] Dash, A. K., Chen, I. M., Yeo, S. H., and Yang G., 2003, "Singularity-Free Path Planning of Parallel Manipulators Using Clustering Algorithm and Line Geometry," *Proceedings of the 2003 IEEE International Conference on Robotics and Automation*, Taipei, Taiwan, Sept. 14–19, pp. 761–766.

[22] Sen, S., Dasgupta, B., and Mallik, A. K., 2003, "Variational Approach for Singularity-Free Path-Planning of Parallel Manipulators," Mech. Mach. Theory, **38**(11), pp. 1165–1183.

[23] Merlet, J.-P., and Daney, D., 2001, "A Formal-Numerical Approach to Determine the Presence of Singularity Within the Workspace of a Parallel Robot," *Proceedings of the International Workshop on Computational Kinematics*, Seoul, May 20–22, pp.167–176.

[24] Tale-Masouleh, M., and Gosselin, C., 2007, "Determination of Singularity-Free Zones in the Workspace of Planar 3-PRR Parallel Mechanisms," ASME J. Mech. Des., **129**(6), pp. 649–652.

[25] Li, H., Gosselin, C., and Richard, M., 2007, "Determination of the Maximal Singularity-Free Zones in the Six-Dimensional Workspace of the General Gough–Stewart Platform," Mech. Mach. Theory, **42**(4), pp. 497–511.